An Extended Differential Flatness Approach for the Health-Conscious Nonlinear Model Predictive Control of Lithium-Ion Batteries

Liu, J; Li, G; Fathy, H

An Extended Differential Flatness Approach for the Health-Conscious Nonlinear Model Predictive Control of Lithium-Ion Batteries

Ji Liu[a], Guang Li[b], and Hosam K. Fathy[a]*

***Abstract*—This article examines the problem of optimizing lithium-ion battery management online, in a health-conscious manner. This is a computationally intensive problem. Previous work by the authors addresses this challenge by exploiting the differential flatness of Fick's law of diffusion to improve computational efficiency, but is limited by the fact that the dynamics of a full battery cell are not differentially flat, even when the individual battery electrode dynamics are. The article addresses this challenge by extending the application of differential flatness to a full single particle model (SPM). Specifically, we use the conservation of charge to express the flat output trajectory of one electrode as an affine function of the other electrode's flat output trajectory. In this way, we enforce differential flatness for the full battery model. This makes it possible to express the battery charge/discharge trajectory in terms of one flat output trajectory. We optimize this trajectory using a pseudospectral method. This reduces the computational cost of the optimization by about a factor of 5 compared to pseudospectral optimization alone. Additionally, the robustness of the nonlinear model predictive control (NMPC) strategy is demonstrated in simulation by adding state of health (SOH) parameter uncertainties.**

***Index Terms*—optimal charging, model predictive control, lithium-ion battery, differential flatness, pseudospectral methods**

I. Introduction

This article proposes a computationally efficient nonlinear model predictive control (NMPC) framework for health-conscious lithium-ion battery management. The article extends previous work by the authors [1], [2] where battery electrode dynamics are shown to be differential flat, and this flatness property is exploited for efficient trajectory optimization. The article's main contribution compared to that work is the fact that it represents the charge dynamics of a full battery cell using a single flat output variable, rather than one flat output variable per electrode. This flat output trajectory is optimized using a pseudospectral method for a reduced-order, electrochemistry-based single particle model (SPM). The use of NMPC can compensate for unmodeled effects [3], which is attractive compared to the implementation of charge/discharge trajectories optimized offline.

Motivation for this article stems from the need to manage lithium-ion battery charging and discharging in a manner that maximizes their power and energy densities while ensuring safety, reliability, and longevity. Traditional battery management systems avoid excessive battery damage and aging by imposing predefined limits on charge/discharge rates, state of charge (SOC), and temperature. This results in simple battery charge/discharge policies, e.g., the constant-current, constant-voltage (CCCV) policy. In contrast, model-based battery control is attractive for two main reasons. First, a model-based controller makes it possible to charge and discharge batteries more aggressively while directly constraining the internal variables (e.g., side reaction overpotentials) associated with aging and degradation. Second, a model-based controller can adapt to battery state of health (SOH), thereby charging/discharging different battery cells with a level of aggressiveness that is consistent with how much they have aged [4]. There is a growing body of research on developing model-based controllers that explore these potential benefits (e.g., [4]–[8]).

There are many challenges associated with model-based battery management, including the need for high-fidelity battery models and accurate battery parameters. This article focuses on alleviating the computational burden associated with model-based battery control. There are two main factors contributing to this computational burden. First, battery management problems involve optimizing the trajectories of battery input current and the internal state variables (such as solid and solution-phase concentrations and potentials). This results in a high computational load, especially for high-fidelity battery models. Second, the dynamics governing battery diffusion, intercalation, and side reactions are often nonlinear and nonconvex. This makes it difficult to employ traditional convex optimization schemes in health-conscious battery control.

The control literature offers a fundamental tool that makes battery trajectory optimization problems significantly more tractable, namely, *differential flatness* [9]. Solid-phase battery diffusion dynamics are governed by Fick's second law of diffusion in each electrode. Fick's law is known to be differentially flat [1], [2]. This concept makes it possible to capture all of the diffusion dynamics in each electrode using one trajectory of a single *flat output* variable instead of all of the state and input variables. Previous work by the authors demonstrates the computational benefits of exploiting differential flatness for battery trajectory optimization. However, one major drawback remains: the dynamics of a full electrochemical battery model are not differentially flat. One way to solve this issue is to exploit time-scale separation by using a battery model which only models the electrode with slower dynamics and neglects the faster dynamics in the other electrode, as shown in [2]. This is not always desirable, since the single-electrode model fails to capture full battery transient dynamics accurately.

This article's novel and unique contribution is the development of an "extended" differential flatness approach for

[a] Department of Mechanical and Nuclear Engineering, Pennsylvania State University, University Park, PA16802, USA

[b] School of Engineering and Material Sciences, Queen Mary, University of London, E1 4NS, United Kingdom

Email: {jxl1081@psu.edu, g.li@qmul.ac.uk, hkf2@psu.edu}

*Address all correspondence to this author.

optimal lithium-ion battery charging and discharging. The proposed extended approach recovers differential flatness by expressing the flat output trajectory of one battery electrode explicitly as a function of the other electrode's flat output. We optimize the flat output trajectories using a computationally efficient pseudospectral method [10]. We perform the optimization within an NMPC framework and demonstrate framework's performance in the presence of parameter uncertainties.

The literature presents several algorithms that can be used for optimizing lithium-ion battery charge/discharge online, in a health-conscious manner. However, the computational burdens associated with these algorithms, such as dynamic programming and genetic algorithms, are prohibitive for model predictive control [11]–[13]. Some researchers alleviate computational burden using the pseudospectral method, and efficient reformulated battery models [8], [14]. While the above tools are valuable, they do not exploit the differential flatness of battery dynamics and the associated computational gains.

The remainder of this article is organized as follows. Section II presents the governing equations and model reduction for the SPM. Section III formulates the health-conscious battery optimal charging problem. Section IV introduces the differential flatness property. In addition, the proposed differential flatness-based Gauss pseudospectral method is introduced in Section V. Section VI shows the results of battery optimal control problem and compares them to an optimized benchmark CCCV protocol. Additionally, the sensitivity of the proposed NMPC framework to parameter uncertainties is studied. Finally, section VII concludes the article.

II. Single Particle Model

In this section, the governing equations of the SPM are presented. The partial differential equations are reduced into ordinary differential equations using orthogonal projection techniques presented in [15]. This article utilizes a physics-based SPM to achieve a reasonable tradeoff between accuracy and computational efficiency [16]–[18]. The parameters of the SPM are obtained from [19] and the reference potential curves for both electrodes are from [20] for a commercial $LiFePO_4$ (LFP) 26650 2.3Ah cell. SPM modeling assumptions can be found in [2].

A. Governing Equations

The governing equations of the SPM are shown below. Solid phase diffusion dynamics are governed by Fick's second law of diffusion. The governing differential equation is

$$\frac{\partial c_j(r,t)}{\partial t} = \frac{D_{s,j}}{r^2}\frac{\partial}{\partial r}\left(r^2\frac{\partial c_j(r,t)}{\partial r}\right) \tag{1}$$

where r is the radial coordinate, t is time, c_j is the lithium-ion concentration in the solid electrode particles, $D_{s,j}$ is the solid phase diffusion coefficient, and $j = p$ corresponds to the positive electrode and $j = n$ to the negative electrode.

The boundary conditions at the particle center ($r = 0$) and particle surface ($r = R_j$) are

$$\frac{\partial c_j(r,t)}{\partial r}\Big|_{r=0} = 0 \tag{2}$$

$$\frac{\partial c_j(r,t)}{\partial r}\Big|_{r=R_j} = -\frac{J_j}{FD_{s,j}a_j} \tag{3}$$

where F is Faraday's number and a_j is the specific interfacial area defined as

$$a_j = \frac{3\varepsilon_j}{R_j} \tag{4}$$

The term R_j is the particle radius and ε_j is active material volume fraction. The molar flux of ions J_i is defined as

$$J_n(t) = -\frac{I(t)}{AL_n} \text{ for negative electrode} \tag{5}$$

$$J_p(t) = \frac{I(t)}{AL_p} \text{ for positive electrode} \tag{6}$$

where I is the input current, defined as positive for charging, A is the battery sheet area, and L_n and L_p are the thicknesses of the negative and positive electrode, respectively.

The bulk state of charge (SOC) is defined as

$$SOC_j(t) = \frac{c_{j,avg}(t)}{c_{j,max}} \tag{7}$$

where $c_{j,max}$ is the maximum concentration of lithium-ions in the electrode and $c_{j,avg}$ is the average lithium-ion concentration in the electrode, i.e.,

$$c_{j,avg}(t) = \int_0^{R_j} c_j(r,t)dr \tag{8}$$

The surface SOC is defined as

$$SOC_j^{surf}(t) = \frac{c_j(t)^{surf}}{c_{j,max}} \tag{9}$$

where c_j^{surf} is the surface lithium-ion concentration.

The Butler-Volmer equation describes the relationship between the molar flux of lithium ions and solid phase potential and can be expressed as

$$J_j(t) = i_{0,j}(t)\left[\exp\left(\frac{\alpha_a F}{RT}\eta_j(t)\right) - \exp\left(-\frac{\alpha_c F}{RT}\eta_j(t)\right)\right] \tag{10}$$

where α_a and α_c are the apparent transfer coefficients, R is the ideal gas constant, T is the cell temperature, and η is the overpotential. The exchange current density i_0 is defined as

$$i_{0,j}(t) = a_j k_j (c_{s,j,\max} - c_j^{surf}(t))^{\alpha_a}(c_j^{surf}(t))^{\alpha_c} c_e^{\alpha_a} \tag{11}$$

where k_j is the reaction rate constant and c_e is the lithium-ion concentration in solution.

The overpotential η_j is defined as the difference between the solid and solution potential minus the open-circuit potential (OCP) of the electrode

$$\eta_j(t) = \phi_{1,j}(t) - \phi_{2,j}(t) - U_j(SOC_j^{surf}(t)) \tag{12}$$

where $\phi_{1,j}$ is the solid phase potential, and $\phi_{2,j}$ is the solution phase potential. The term U_j is the OCP as a function of the

surface SOC. The reference potential curves are obtained from [21].

The potential drop in the solution phase between two electrodes is

$$\phi_{2,p}(t) - \phi_{2,n}(t) = I(t)R_{cell} \tag{13}$$

where R_{cell} is a lumped parameter which captures the effective resistance of the solution. Details can be found in [1].

The cell voltage is defined as the difference in potential between the positive and negative electrode

$$V(t) = \phi_{1,p}(t) - \phi_{1,n}(t) \tag{14}$$

This article adopts a physics-based side reaction constraint from [22] for health-conscious optimal charging. This side reaction represents lithium plating and can be expressed as

$$\eta_{sr}(t) = \phi_{1,n}(t) - \phi_{2,n}(t) - U_{sr}(c_n^{surf}(t)) \geq 0 \tag{15}$$

where η_{sr} is the side reaction overpotential and $U_{sr}(c_n^{surf})$ denotes the reference potential of the side reaction and is zero for lithium-ion batteries [4].

B. Model Reduction

This article adopts an efficient Legendre polynomial-based orthogonal projection method. We approximate the lithium ion concentration profile $c_j(r,t)$ along the particle radius using as a linear combination of some unknown coefficients $\beta_j(t)$ (as functions of time t) and known Legendre polynomials $P_{j,i}(r)$ with degree i (as a function of radius r)

$$c_j(r,t) \approx \sum_{i=0}^{M} \beta_{j,i}(t) P_{j,i}(r) \tag{16}$$

where M is the degree of Legendre polynomials and is an even integer to satisfy the boundary condition (2), $P_{j,i}$ is the i-th degree Legendre polynomial corresponding to the term c_j for electrode j, and $\beta_{j,i}(t)$ is the i-th unknown coefficient for electrode j.

The Legendre polynomials are normalized such that

$$\int_0^{R_j} P_{j,i}(r) P_{j,k}(r) dr = \begin{cases} 0 & \text{if } i \neq k \\ 1 & \text{if } i = k \end{cases} \tag{17}$$

where R_j is the radius of particles.

Substituting Eq. (16) into Eq. (1) gives

$$\begin{aligned} &\sum_{i=0}^{M} P_{j,i}(r)\dot{\beta}_{j,i}(t) \\ &= D_{s,j}\left[\frac{2}{r}\sum_{i=0}^{M}\frac{dP_{j,i}(r)}{dr}\beta_{j,i}(t) + \sum_{i=0}^{M}\frac{d^2P_{j,i}(r)}{dr^2}\beta_{j,i}(t)\right] \end{aligned} \tag{18}$$

where $\dot{\beta}_{j,i}(t)$ is the derivative with respect to time.

Galerkin projection is used to get the unknown coefficients $\beta_{j,i}(t)$. This is achieved by multiplying both sides of (18) by $P_{j,i}(r)$ and integrating over the radial coordinate. This furnishes the dynamics of the coefficients $[\beta_{j,0}, \beta_{j,2}, \ldots, \beta_{j,M}]^T$.

The number of Legendre polynomials decides the accuracy and the efficiency of the model reduction method and we choose $M = 6$ in this article. The diffusion dynamics Eq. (1) in each electrode can then be expressed as follows

$$\begin{bmatrix}\dot{\beta}_{j,0}\\ \dot{\beta}_{j,2}\\ \dot{\beta}_{j,4}\\ \dot{\beta}_{j,6}\end{bmatrix} = \frac{D_{s,j}}{R_j^2}\begin{bmatrix}0, & 9\sqrt{5}, & 20, & 29.4\sqrt{13}\\ 0, & 0, & 35\sqrt{5}, & 16.8\sqrt{65}\\ 0, & 0, & 0, & 46.2\sqrt{13}\\ 0, & 0, & 0, & 0\end{bmatrix}\begin{bmatrix}\beta_{j,0}\\ \beta_{j,2}\\ \beta_{j,4}\\ \beta_{j,6}\end{bmatrix} \tag{19}$$

Similarly, the boundary condition Eq. (3) can be expressed as

$$\begin{aligned} \frac{3}{R_j}\sqrt{\frac{5}{2R_j}}\beta_{j,2}(t) + \frac{10}{R_j}\sqrt{\frac{9}{2R_j}}\beta_{j,4}(t) + \frac{21}{R_j}\sqrt{\frac{13}{2R_j}}\beta_{j,6}(t) \\ = -\frac{J_j}{D_{s,j}a_j} \end{aligned} \tag{20}$$

From Eq. (19) and Eq. (20), it can be seen that the term $\beta_{j,6}$ does not have dynamics and can be expressed as a function of other unknown variables. Therefore, it is not considered as a state variable. As a result, we achieve a standard state-space representation for the dynamics of the electrode j

$$\dot{x}_j(t) = A_j x_j(t) + B_j u(t) \tag{21}$$

where state vector for electrode j is

$$x_j = [\beta_{j,0}(t), \beta_{j,2}(t), \beta_{j,4}(t)]^T \tag{22}$$

$x_j \in R^3$ and input is $u \in R^1$. From Eq. (23), the diffusion dynamics in each electrode in the SPM are decoupled. Therefore, the state space representation of full SPM dynamics can be expressed as

$$\dot{x}(t) = Ax(t) + Bu(t) \tag{23}$$

where $x_j \in R^{n_x}$ and $u \in R^{n_u}$. In this article, the state variables are

$$\begin{aligned} x(t) &= [x_n^T(t), x_p^T(t)]^T \\ &= [\beta_{n,0}(t), \beta_{n,2}(t), \beta_{n,4}(t), \beta_{p,0}(t), \beta_{p,2}(t), \beta_{p,4}(t)]^T \end{aligned} \tag{24}$$

and the input u is the applied current, i.e., $u(t) = I(t)$. Therefore, $n_x = 6$ and $n_u = 1$. The state matrix is

$$A = \begin{bmatrix} A_n & \mathbf{0} \\ \mathbf{0} & A_p \end{bmatrix} \tag{25}$$

where $\mathbf{0}$ is a 3×3 zero matrix and the input matrix is

$$B = \begin{bmatrix} B_n \\ B_p \end{bmatrix} \tag{26}$$

III. Problem Formulation

The proposed NMPC framework can be applied to solve general battery trajectory optimization problems, such as optimal charging and discharging in the presence of different aging and degradation constraints. In the remainder of this article, we focus on optimal charging in the presence of a lithium plating side reaction constraint as an illustrative example, and our focus on charging (rather than discharging) is justified by the fact that plating is more likely to occur during charging.

The problem is formulated as follows

$$\begin{aligned}\min_{u} J = &\int_{t_0}^{t_f} \left(SOC_n(t) - SOC_{ref}\right)^2 dt \\ \text{s.t: model Eq. } (7)-(12),&(15),(16),(23) \\ &0 \le u(t) \le u_{\max} \\ &\eta_{sr}(t) \ge 0 \\ &SOC_n(0) = SOC_{ini}\end{aligned} \tag{27}$$

The goal of this problem is to bring battery state of charge to a level as close as possible to some target, SOC_{ref}, given the initial SOC, SOC_{ini}, within the time duration $[t_0, t_f]$. This optimization problem is subject to constraints imposed by: battery dynamics, maximum and minimum current limitations, and the desire to avoid side reaction overpotentials conducive to lithium plating. The side reaction constraint Eq. (15) distinguishes the problem from the traditional CCCV strategy which charges batteries using pre-determined voltage and input constraints. Additionally, the side reaction overpotential η_{sr} in Eq. (15) is a nonlinear and nonconvex function with respect to x and u.

We solve the above optimization problem using NMPC. The nonlinearity of the optimization problem is mainly due to the side reaction constraint (15). The input charging trajectory is optimized at each sampling time and only the first value of this trajectory is utilized. The optimization is then repeated using the updated state variables at the next sampling time. The use of the NMPC strategy can compensate for uncertainties (e.g., parameter uncertainty) and noise by re-optimizing the problem at each sampling time, which is demonstrated in Section VI-C. Due to the complexity of the NMPC problem, stability analysis is beyond the scope of this article. Note that the optimization problem assumes that all SPM state variables are known. Battery parameter and state estimation is an interesting research topic that is already addressed extensively in the literature [23]–[25].

IV. Differentially Flat Systems

A. Introduction

Mathematically, a system is *differentially flat* if there exists a *flat output* z such that [9], [26]:

1) the state x and input u can be expressed in terms of the flat output z and a finite number of its derivatives as

$$x = f_x(z, \dot{z}, \ldots, z^{(\alpha)}) \tag{28a}$$
$$u = f_u(z, \dot{z}, \ldots, z^{(\beta)}) \tag{28b}$$

2) the flat output z can be expressed in terms of state x, input u, and a finite number of input's derivatives

$$z = f_z(x, u, \dot{u}, \ldots, u^{(\gamma)}), \tag{29}$$

where α, β, γ are positive integers that depend on the order of the model and $z^{(r)}$ is the r^{th} derivative with respect to time. The flat outputs are equal in number to the input variables.

B. Application to Batteries

Differential flatness can be seen as an extension of the concept of controllability to nonlinear systems. In fact, for linear systems, a system is differentially flat if and only if it is controllable [27]. The diffusion dynamics in each battery electrode are controllable and hence differentially flat. As a result, only one flat output trajectory is required to represent the system dynamics in each electrode. The state and input variables can then be recovered using the flat output trajectory according to Eq. (28). Therefore, the application of differential flatness makes it possible to represent battery dynamics in a computationally efficient manner.

The flat output for the electrode j, z_j, is found by transforming the reformulated diffusion sub-model for each electrode into the controllable canonical form. One can define the flat output as the first transformed state:

$$z_j(t) := \bar{x}_{j,1}(t) \tag{30}$$

where $\bar{x}_j$ is transformed state vector for the sub-model of electrode j.

The transformed state variables $\bar{x}_j$ can then be expressed using the flat output and a finite number of its derivatives. Therefore, the original state variables x_j can be expressed by

$$x_j(t) = f_x(z_j(t), \dot{z}_j(t), \ddot{z}_j(t)) = Q \left(\begin{bmatrix} 1 & 0 & 0 \\ 0 & 1 & 0 \\ 0 & 0 & 1 \end{bmatrix} \begin{bmatrix} z_j(t) \\ \dot{z}_j(t) \\ \ddot{z}_j(t) \end{bmatrix} \right) \tag{31}$$

where Q is the transformation matrix for the controllable canonical form and the product in parentheses is the transformed state $\bar{x}_j$. The input can be expressed similarly as well

$$\begin{aligned} u(t) &= f_u(z_j(t), \dot{z}_j(t), \ddot{z}_j(t), \dddot{z}_j(t)) \\ &= [-\alpha_{j,1}, -\alpha_{j,2}, -\alpha_{j,3}, 1] \begin{bmatrix} z_j(t) \\ \dot{z}_j(t) \\ \ddot{z}_j(t) \\ \dddot{z}_j(t) \end{bmatrix} \end{aligned} \tag{32}$$

where $\alpha_{j,i}$ are the coefficients of characteristic equation of the state matrix A_j in Eq. (25).

V. Flatness-Based Gauss Pseudospectral Method

Pseudospectral methods are a class of direct methods which transform the original problem into a nonlinear programming (NLP) problem that can be solved using well-developed NLP algorithms. The Gauss pseudospectral method (GPM) is adopted in this article. The collocation points τ_i in the GPM are the Legendre-Gauss (LG) points which are the roots of N^{th} degree Legendre polynomials $P_N(\tau_i)$ and are located in the interior of the range $[-1, 1]$, i.e., $\tau_i \in (-1, 1)$ [10]. The discretization points are collocation points plus the boundaries, i.e., $\tau_0 = -1$ and $\tau_{N+1} = 1$. The remainder of this section describes how to use the GPM to optimize the flat output trajectory for differentially flat systems.

First, the time $t \in [t_0, t_f]$ needs to be mapped into τ domain to use collocation points

$$t = \frac{(t_f - t_0)\tau + (t_f + t_0)}{2} \tag{33}$$

The GPM approximates the trajectories of flat output as a linear combination of $N+1$ Lagrange polynomials at N collocation points and the initial point $\tau_0 = -1$. The flat output z_j (the subscript represents the electrode j) is approximated

$$z_j(\tau) \approx \mathbf{z}_j(\tau) = \sum_{k=0}^{N} L_k(\tau) z_j(\tau_k) \tag{34}$$

where $\mathbf{z}_j(\tau)$ is the approximated trajectory of the flat output in the electrode j and $L_k(\tau)$ is the Lagrange polynomial bases. The property of Lagrange polynomials leads to

$$\mathbf{z}_j(\tau_k) = z_j(\tau_k) \tag{35}$$

as stated in [1].

One benefit of using pseudospectral methods is that one can express the derivatives of variables analytically by differentiating Eq. (34). The first derivative of the flat output evaluated at collocation points gives

$$\mathbf{z}_j^{(l)}(\tau_i) = \sum_{k=0}^{N} L_k^{(l)}(\tau_i) \mathbf{z}_j(\tau_k) \tag{36}$$

where the term $L_k^l(\tau_i)$ represents the l-th derivative of Lagrange polynomials evaluated at time τ_i and can be expressed using the differentiation matrix $D_l(i,k) = L_k^{(l)}(\tau_i)$.

Therefore, the l-th derivative of the flat output in Eq. (36) can be expressed using a more compact way

$$Z_j^{(l)} = D_l Z_j \tag{37}$$

where $Z_j := [\mathbf{z}_j(\tau_0), \mathbf{z}_j(\tau_1), \cdots, \mathbf{z}_j(\tau_N)]^T$ and $Z_j^{(l)}$ is a vector of the l-th derivative of $\mathbf{z}_j(\tau_i)$. Therefore, the following equations holds $\bar{X}_{j,1} = Z_j$, $\bar{X}_{j,2} = D_1 Z_j$, and $\bar{X}_{j,3} = D_2 Z_j$, where $\bar{X}_{j,k} := [\bar{\mathbf{x}}_{j,k}(\tau_1), \bar{\mathbf{x}}_{j,k}(\tau_2), \cdots, \bar{\mathbf{x}}_{j,k}(\tau_N)]^T$.

As a result, the trajectory of the state x_j evaluated at collocation points can be expressed using the flat output trajectory with Eq. (31). Equation (32) provides the mapping from z_j to u

$$\begin{aligned} U &:= [u(\tau_0), u(\tau_1), \cdots, u(\tau_N)]^T \\ &= -\alpha_{j,1} I_N Z_j - \alpha_{j,2} D_1 Z_j - \alpha_{j,2} D_2 Z_j - \alpha_{j,3} D_3 Z_j \end{aligned} \tag{38}$$

where I_N is a identity matrix.

Moreover, pseudospectral methods integrate the cost function J using the LG quadrature rule

$$\begin{aligned} J &= \int_{t_0}^{t_f} \left(SOC_n(\tau) - SOC_{ref}\right)^2 d\tau \\ &\approx \frac{t_f - t_0}{2} \sum_{i=1}^{N} w_i \left(SOC_n(\tau_i) - SOC_{ref}\right)^2 \\ &= \frac{t_f - t_0}{2} \sum_{i=1}^{N} w_i L_z(Z_n, Z_p, \tau_i) \end{aligned} \tag{39}$$

with $[Z_n^T, Z_p^T]^T$ as a vector consisting of optimization variables and $\mathcal{L}_{z,i}(\cdot)$ is the cost function evaluated at i$^{\text{th}}$ collocation point. The Gauss weights w_i are determined by

$$w_i = \frac{2}{1 - \tau_i^2} \left[\dot{P}_N(\tau_i)\right]^2 \tag{40}$$

The term $\dot{P}_N(\tau_i)$ is the first derivative of the N$^{\text{th}}$ degree of Legendre polynomials $P_N(\tau_i)$ evaluated at collocation point τ_i.

The inequality constraints can also be expressed as a function of the optimization variables

$$\mathcal{C}(Z_n, Z_p) \leq 0 \tag{41}$$

A. Two Flat Outputs Approach

In authors' previous work [1], two flat outputs are required for the optimization problem (27). The resulting optimization problem with the application of differential flatness is shown as follows

$$\begin{aligned} \min_{Z_n, Z_p} \; & J = \int_{t_0}^{t_f} \left(SOC_n(t) - SOC_{ref}\right)^2 dt \\ \text{s.t: } & \text{model Eq. } (7) - (12), (15), (16), (31), (32) \\ & u_n(\tau_i) = u_p(\tau_i) \\ & 0 \leq u(\tau_i) \leq u_{\max} \\ & \eta_{sr}(\tau_i) \geq 0, \text{ where } i = 1, 2, \cdots, N \\ & SOC_n(0) = SOC_{ini} \end{aligned} \tag{42}$$

This problem formulation explicitly optimizes the trajectories of both z_n and z_p, subject to model dynamics and inequality constraints. The term N is the number of collocation points in the prediction horizon. Additionally, unlike the formulation in problem (27), there is no explicit model dynamic constraint Eq. (23). This is because model dynamics are automatically satisfied by exploiting the flatness property using Eq. (31) and Eq. (32). Note that there is an extra equality constraint on the current in each electrode, which is required to satisfy the conservation of charge.

B. Extended Differential Flatness Approach

While the approach described above is efficient, it is necessary to use two trajectories of the flat outputs, $z_n(t)$ and $z_p(t)$, to represent full battery dynamics. This doubles the number of optimization variables needed for determining the optimal battery trajectory, and also introduces linear equality constraints between these variables. In contrast, this article shows that the dynamics of the entire battery can be forced to be differentially flat for the first time. Typically, the battery only has one input, i.e., the input current, and hence one flat output variable is enough to represent the dynamics of the entire SPM. We achieve this using the law of conservation of charge: the amount of charge transferring through each electrode per unit time is the same, and therefore the current through both electrodes is the same

$$u_n(t) = u_p(t) \tag{43}$$

Equation (38) and (43) give the relationship between the flat output Z_p and Z_n

$$\begin{aligned} Z_p = &\left(-\alpha_{p,1} - \alpha_{p,2} D_1 - \alpha_{p,2} D_2 - \alpha_{p,3} D_3\right)^{-1} \\ &\left(-\alpha_{n,1} - \alpha_{n,2} D_1 - \alpha_{n,2} D_2 - \alpha_{n,3} D_3\right) Z_n \end{aligned} \tag{44}$$

While the matrix inversion in Eq. (44) takes some computational time, this matrix inversion can be performed offline a

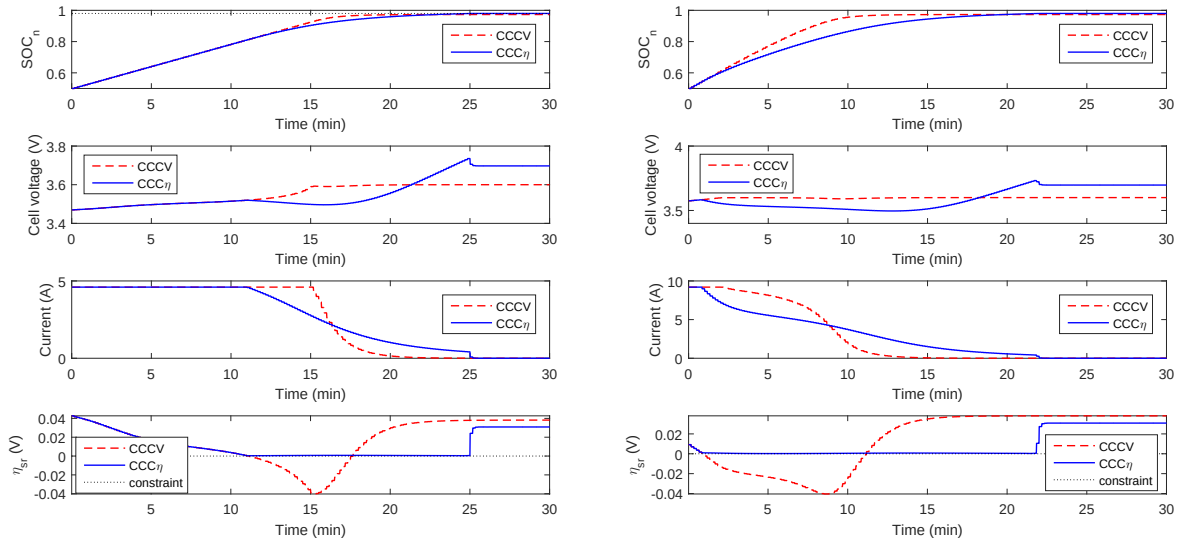

(a) $u_{\max} = 4.6A$ (2C)

(b) $u_{\max} = 9.6A$ (4C)

Fig. 1: Comparison of two charging strategies: health-conscious optimal charging pattern (CCCη) from problem (27) versus CCCV charging pattern from problem (46). The CCCη charging can protect the cell from lithium plating side reaction.

priori, and does not affect the computational burden of online MPC. As a result, the problem (27) can be formulated and solved in a more efficient way

$$\begin{aligned} \min_{Z_n} J &= \int_{t_0}^{t_f} \left(SOC_n(t) - SOC_{ref}\right)^2 dt \\ \text{s.t: model Eq. } &(7)-(12),(15),(16),(31),(32),(44) \\ & 0 \le u(\tau_i) \le u_{\max} \\ & \eta_{sr}(\tau_i) \ge 0 \text{ where } i = 1, 2, \cdots, N \\ & SOC_n(0) = SOC_{ini} \end{aligned} \tag{45}$$

This problem formulation only requires the optimization of Z_n, the flat output variable z_n evaluated at each collocation point. Therefore, the resulting optimization problem using the extended approach only needs half of the optimization variables and no equality constraints compared to the NLP in Eq. (42). This makes the proposed framework computationally very efficient.

VI. Results and Discussion

A. Results of Online Health-Conscious Optimal Charging

Problem (27) is set to start at $t_0 = 0$ with the initial SOC as 0.5 and with the sampling time as 10s (i.e., $\Delta t = 10s$). The sampling time is chosen such that it is about 5 times faster than the fastest time constant (about 60s). But the sampling time can be smaller. The prediction horizon is $T_p = 100s$ and at each time step the optimization problem is solved with 4 collocation points, i.e., $N = 4$. Due to the computational benefits, the proposed NMPC framework is able to solve the problem during each sampling time. The hot-start strategy is used: the solution of previous sampling instance is used as the starting point (i.e., initial guess) for the current problem. All of simulations are solved in MATLAB using the "Fmincon" function on a laptop with a 2.4GHz CPU.

Figure 1 depicts the results of problem (27) using two current upper bounds. Focusing on Fig. 1b, i.e., the trajectory with $u_{\max} = 9.6A$ (i.e., 4C where 1C corresponds to 2.3A current), one can see the input trajectory first charges the battery with the maximum rate, because when a cell has low SOC the overpotential of lithium plating (15) can be positive even with high current. This is due to the fact that batteries at low SOC tend to have high positive reference potential. Once the side reaction constraint reaches zero, the charging current is tapered to satisfy the side reaction constraint. This charging process terminates when the battery SOC reaches the desired SOC. From the results, one can see the charging profiles have the following pattern: batteries are charged first with constant maximum current rate and then the current is decreased to keep constant overpotential. We call this charging profile as constant current constant overpotential (CCCη) strategy. The other trajectory shown in Fig. 1a demonstrates a similar pattern as described above.

B. Traditional CCCV Charging

To compare with the health-conscious optimal charging results, this article also solves a standard CCCV charging problem with only voltage and current limits

$$\begin{aligned} \min_{u} J &= \int_{t_0}^{t_f} \left(SOC_n(t) - SOC_{ref}\right)^2 dt \\ \text{subject to: model Eq. } &(7)-(14),(16),(23) \\ & 0 \le u(t) \le u_{\max} \\ & V(t) \le V_{\max} \end{aligned} \tag{46}$$

where this problem has the same SOC reference and current limits as problem (27) and $V_{\max}$ is voltage limit. The problem is solved using the proposed NMPC framework with $\Delta t = 10s$, $T_p = 100s$, $V_{\max} = 3.6V$ and $N = 4$.

The dashed lines in Fig. 1 depicts the simulation results of problem (46): the traditional CCCV strategy. The optimal charging current first charges the battery with the constant maximum charging rate until the voltage upper limit is reached. Then voltage is kept as constant by charging the battery using reduced current. Note that while the side reaction overpotential is shown in Fig. 1, it is not considered as a constraint in the optimization.

The benefits of health-conscious battery optimal charging can be seen by comparing two charging trajectories in either Fig. 1a or Fig. 1b. The side reaction overpotentials are negative for substantial durations of time for CCCV charging. Therefore, CCCV charging can lead to excessive lithium-ion loss through lithium plating. The charging patterns in problem (27), i.e., the CCCη charging, however, can charge the battery without excessive degradation and reach the targeted charge capacity at the same time, even if the current upper limit is set to be aggressive.

C. NMPC Sensitivity to Parameter Uncertainties

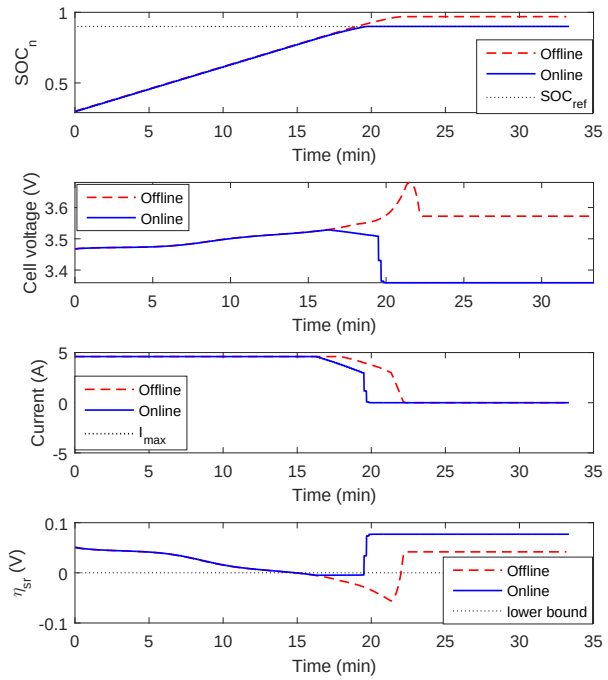

Fig. 2: The NMPC framework is more robust than offline framework.

This article demonstrates the robustness of the proposed NMPC framework with respect to SOH parameters by comparing with an offline optimal charging solution. The volume fraction of the active material ε_j in Eq. (4) is one of the SOH parameters relating to electrode capacity in SPM and hence cell capacity, which changes with aging for a given battery [28]. Suppose the controller assumes each electrode has its original capacity, while the actual capacity is only 90% of the original due to aging.

Figure 2 demonstrates the robustness of the NMPC framework. Both online and offline solutions do violate lithium plating overpotential constraints due to the uncertain SOH parameter ε_j. However, the online solution has much smaller lithium plating overpotential violation over a shorter duration and therefore exhibits less lithium plating. This is because the NMPC framework updates the optimal trajectory at every sampling time based on the updated state variables.

D. Comparison of Three NMPC Frameworks

TABLE I: Comparison of 3 NMPC frameworks: The proposed framework is the most efficient.

NMPC Framework	Optimization variables	Equality constraints
GPM	$(n_x + n_u) \times N = 7N$	$n_x \times N = 6N$
Two flat outputs GPM	$2n_u \times N = 2N$	$n_u \times N = N$
One flat output GPM	$n_u \times N = N$	0

The efficiency of the proposed framework in this article is demonstrated by solving problem (27) online using 3 approaches: i) the GPM, ii) the flatness-based GPM with two flat outputs shown in problem (42) (differential flatness only applies to each electrode but not the entire battery), and iii) the flatness-based GPM with one flat output in problem (45) (the one proposed in this article). All three simulations are conducted using the same set of parameters (i.e., $\Delta t = 5s$, $T_p = 400s$, $SOC(t_0) = 0.4$, $t_0 = 0s$, and $t_f = 2100s$). Figure 3 depicts the average simulation time for one time step as a function of the number of collocation points. The average simulation time is calculated by dividing the simulation time for the entire optimization by the number of time steps. While all three approaches produce the same charging profile, the extended flatness-based approach proposed in this paper can reduce the computational time by abut a factor of 5 compared to online pseudospectral optimization alone.

The proposed NMPC framework is computationally efficient mainly for two reasons. First, by using the differential flatness property, it automatically satisfies system dynamic constraints. Therefore the resulting NLP problem does not have any explicit dynamic constraints. This holds for both methods using differential flatness. Second, the proposed extended flatness-based method reduces the number of optimization variables significantly. Specifically, the proposed extended flatness-based method only requires N optimization variables, since the differential flatness for the full SPM is recovered.

VII. Conclusions

This article proposes a computationally efficient nonlinear model predictive control (NMPC) framework to solve battery trajectory optimization problem online. This framework extends the differential flatness approach to recover the flatness of the single particle battery model, which makes it possible to represent the dynamics of the entire battery using only one flat output. The trajectory of the resulting flat output is optimized

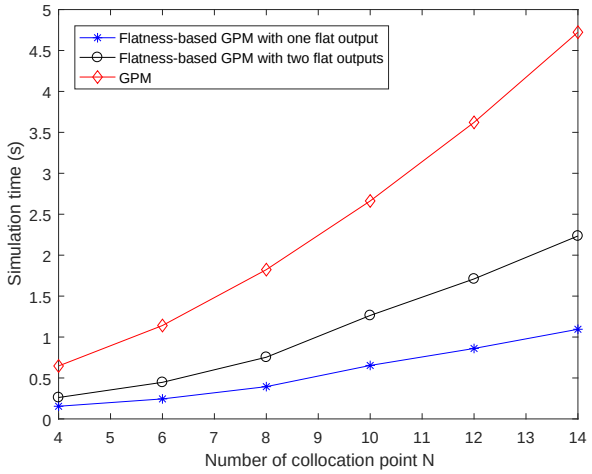

Fig. 3: Average simulation time for each time step. The proposed extended flatness approach is more efficient than the flatness-based GPM with two flat outputs proposed in [1].

using pseudospectral methods. This article demonstrates the proposed NMPC framework by applying it to solve an online health-conscious battery optimal charging problem with a physics-based side reaction constraint. The optimal charging strategy is shown to follow the pattern of constant current constant side reaction overpotential (CCCη). The robustness of the NMPC framework is demonstrated for specific SOH parameter uncertainties. The proposed framework improves computational efficiency by a factor of 5 compared to pseudospectral optimization alone.

Acknowledgement

The research was funded by ARPA-E AMPED program grant # 0675-1565. The authors gratefully acknowledge this support.

References

[1] J. Liu, G. Li, and H. K. Fathy, "Efficient lithium-ion battery model predictive control using differential flatness-based pseudospectral methods," in *ASME 2015 Dynamic Systems and Control Conference*. American Society of Mechanical Engineers, 2015, pp. V001T13A005–V001T13A005.

[2] J. Liu, G. Li, and H. K. Fathy, "A computationally efficient approach for optimizing lithium-ion battery charging," *Journal of Dynamic Systems, Measurement, and Control*, vol. 138, no. 2, p. 021009, 2016.

[3] Y. Fang and A. Armaou, "Nonlinear model predictive control using a bilinear carleman linearization-based formulation for chemical processes," in *American Control Conference (ACC), 2015*. IEEE, 2015, pp. 5629–5634.

[4] N. A. Chaturvedi, R. Klein, J. Christensen, J. Ahmed, and A. Kojic, "Modeling, estimation, and control challenges for lithium-ion batteries," in *American Control Conference (ACC)*. IEEE, 2010, pp. 1997–2002.

[5] S. K. Rahimian, S. Rayman, and R. E. White, "Optimal charge rates for a lithium ion cell," *Journal of Power Sources*, vol. 196, no. 23, pp. 10 297–10 304, 2011.

[6] H. Fang and Y. Wang, "Health-aware and user-involved battery charging management for electric vehicles using linear quadratic control," in *ASME 2015 Dynamic Systems and Control Conference*. American Society of Mechanical Engineers, 2015, pp. V001T13A009–V001T13A009.

[7] S. Moura, N. Chaturvedi, and M. Krstic, "Constraint management in li-ion batteries: A modified reference governor approach," in *American Control Conference (ACC), 2013*. IEEE, 2013, pp. 5332–5337.

[8] X. Hu, H. E. Perez, and S. J. Moura, "Battery charge control with an electro-thermal-aging coupling," in *ASME 2015 Dynamic Systems and Control Conference*. American Society of Mechanical Engineers, 2015, pp. V001T13A002–V001T13A002.

[9] M. Fliess, J. Lévine, P. Martin, and P. Rouchon, "Flatness and defect of non-linear systems: introductory theory and examples," *International journal of control*, vol. 61, no. 6, pp. 1327–1361, 1995.

[10] G. T. Huntington, "Advancement and analysis of a Gauss pseudospectral transcription for optimal control problems," Ph.D. dissertation, Citeseer, 2007.

[11] S. J. Moura, J. C. Forman, S. Bashash, J. L. Stein, and H. K. Fathy, "Optimal control of film growth in lithium-ion battery packs via relay switches," *Industrial Electronics, IEEE Transactions on*, vol. 58, no. 8, pp. 3555–3566, 2011.

[12] S. Bashash, S. J. Moura, J. C. Forman, and H. K. Fathy, "Plug-in hybrid electric vehicle charge pattern optimization for energy cost and battery longevity," *Journal of Power Sources*, vol. 196, no. 1, pp. 541–549, 2011.

[13] A.-A. Mamun, I. Narayanan, D. Wang, A. Sivasubramaniam, and H. K. Fathy, "Multi-objective optimization to minimize battery degradation and electricity cost for demand response in datacenters," in *Dynamic Systems and Control Conference*. ASME, 2015.

[14] R. Methekar, V. Ramadesigan, R. D. Braatz, and V. R. Subramanian, "Optimum charging profile for lithium-ion batteries to maximize energy storage and utilization," *ECS Transactions*, vol. 25, no. 35, pp. 139–146, 2010.

[15] M. A. Kehs, M. D. Beeney, and H. K. Fathy, "On the solution of the DFN battery model using descriptor form with Legendre and Galerkin projections," 2014, to be presented at American Control Conference.

[16] V. Ramadesigan, P. W. Northrop, S. De, S. Santhanagopalan, R. D. Braatz, and V. R. Subramanian, "Modeling and simulation of lithium-ion batteries from a systems engineering perspective," *Journal of The Electrochemical Society*, vol. 159, no. 3, pp. R31–R45, 2012.

[17] C. Manzie, C. Zou, and D. Nesic, "Simplification techniques for pde-based li-ion battery models," in *2015 54th IEEE Conference on Decision and Control (CDC)*, Dec 2015, pp. 3913–3921.

[18] C. Zou, C. Manzie, and D. Nei, "A framework for simplification of pde-based lithium-ion battery models," *IEEE Transactions on Control Systems Technology*, vol. PP, no. 99, pp. 1–16, 2015.

[19] J. C. Forman, S. J. Moura, J. L. Stein, and H. K. Fathy, "Genetic parameter identification of the doyle-fuller-newman model from experimental cycling of a lifepo 4 battery," in *American Control Conference (ACC), 2011*. IEEE, 2011, pp. 362–369.

[20] M. Safari and C. Delacourt, "Modeling of a commercial graphite/lifepo4 cell," *Journal of the Electrochemical Society*, vol. 158, no. 5, pp. A562–A571, 2011.

[21] A. Funabiki, M. Inaba, Z. Ogumi, S.-i. Yuasa, J. Otsuji, and A. Tasaka, "Impedance study on the electrochemical lithium intercalation into natural graphite powder," *Journal of the Electrochemical Society*, vol. 145, no. 1, pp. 172–178, 1998.

[22] R. Klein, N. Chaturvedi, J. Christensen, J. Ahmed, R. Findeisen, and A. Kojic, "Optimal charging strategies in lithium-ion battery," in *American Control Conference (ACC), 2011*, 2011, pp. 382–387.

[23] S. Dey, B. Ayalew, and P. Pisu, "Combined estimation of state-of-charge and state-of-health of li-ion battery cells using smo on electrochemical model," in *2014 13th International Workshop on Variable Structure Systems (VSS)*. IEEE, 2014, pp. 1–6.

[24] R. Xiong, F. Sun, Z. Chen, and H. He, "A data-driven multi-scale extended kalman filtering based parameter and state estimation approach of lithium-ion olymer battery in electric vehicles," *Applied Energy*, vol. 113, pp. 463–476, 2014.

[25] B. Xia, X. Zhao, R. De Callafon, H. Garnier, T. Nguyen, and C. Mi, "Accurate lithium-ion battery parameter estimation with continuous-time system identification methods," *Applied Energy*, vol. 179, pp. 426–436, 2016.

[26] J. Oldenburg and W. Marquardt, "Flatness and higher order differential model representations in dynamic optimization," *Computers & chemical engineering*, vol. 26, no. 3, pp. 385–400, 2002.

[27] G. Li, "Nonlinear model predictive control of a wave energy converter based on differential flatness parameterisation," *International Journal of Control*, pp. 1–10, 2015.

[28] J. Liu, M. Rothenberger, S. Mendoza, P. Mishra, Y.-s. Jung, and H. K. Fathy, "Can an identifiability-optimizing test protocol improve the robustness of subsequent health-conscious lithium-ion battery control? an illustrative case study," in *2016 American Control Conference (ACC)*. IEEE, 2016, pp. 6320–6325.